

## X-ray and gamma-ray study for 2023 nova eruption of V1716 Sco

H.-H. WANG,<sup>1</sup> H.-D. YAN,<sup>2</sup> J. TAKATA,<sup>2</sup> AND L.C.-C., LIN<sup>3</sup>

<sup>1</sup>*School of Physics and Engineering, Henan University of Science and Technology, Luoyang 471023, China*

<sup>2</sup>*Department of Astronomy, School of Physics, Huazhong University of Science and Technology, Wuhan 430074, China*

<sup>3</sup>*Department of Physics, National Cheng Kung University, Tainan 701401, Taiwan*

### ABSTRACT

We report the results of X-ray and gamma-ray analyses of the nova V1716 Sco taken by *Swift*, *NICER*, *NuSTAR* and *Fermi-LAT*. We have detected gamma-ray emission at a significant level exceeding  $8\sigma$  in daily bins starting the day after the optical eruption. The gamma-ray emission, characterized by a Test Statistic (TS) value more than four, persisted for approximately 40 days. Notably, harder X-ray emission were observed by *NuSTAR* as the start of gamma-ray emission, which is the fourth classical nova that gamma-ray emission is concurrent with harder X-ray emission from *NuSTAR* data. V1716 Sco is one of rare samples that clearly shows a hard X-ray emission (1-10 keV bands) in the *Swift-XRT* data concurrently with gamma-ray emission of *Fermi-LAT* data, and its light curve in 1.0-10.0 keV bands had a peak at about 20 days after the optical eruption. The X-ray spectrum was initially fitted by a model of thermal plasma emission, and entered a supersoft phase with additional blackbody (BB) component emerged around about 40 days after the optical eruption. *NICER* data taken in supersoft source phase revealed a quasi-periodic oscillation with a period of  $79.10 \pm 1.98$  seconds, and the peak phase of the folded light curve varied with time. Moreover, V1716 Sco is the another example that the emission radius in supersoft source phase is significantly larger than the radius of white dwarf, and a simple BB emission model may not be applicable since the luminosity exceeds significantly Eddington limit.

*Keywords:* nova, V1716 Sco – stars: novae, cataclysmic variables – stars: white dwarfs

### 1. INTRODUCTION

Classical novae are thermonuclear eruptions that occur in binary systems, where a white dwarf (hereafter WD) accretes matter from its companion. The energy released from the thermonuclear eruption causes a dramatic expansion and ejection of the accreted envelope. Observations have shown that the ejected matter expands into the surrounding environment at speeds ranging from hundreds to thousands of  $\text{km s}^{-1}$  (Gallagher & Starrfield 1978) and have confirmed multi-wavelength emission from radio to TeV gamma-ray bands (Chomiuk et al. 2021; Acciari et al. 2022; H. E. S. S. Collaboration et al. 2022). Hard X-ray and gamma-ray emissions are thought to be evidence of the formation of the shock

due to the novae outflows (Metzger et al. 2014). The *Fermi* Large Area Telescope (hereafter *Fermi-LAT*) has confirmed GeV emissions from 20 novae and potential emissions from 6 sources, since its launch in 2008<sup>1</sup>. It is argued that the collisions of the multiple ejecta (internal shock) or the interaction between the ejecta and preexisting medium surrounding the binary can cause the shock (Della Valle & Izzo 2020; Aydi et al. 2020; Chomiuk et al. 2021), resulting in the production of gamma-rays through leptonic and/or hadronic processes (e.g. Vurm & Metzger 2018; Chomiuk et al. 2021). Most novae detected in the GeV range are classified as classical novae, typically having a main-sequence star as the companion. These shocks are thought to be internal, resulting from collisions of the multiple ejecta (Metzger et al. 2014).

wanghh33@mail.sysu.edu.cn

yanhdhh@hust.edu.cn

takata@hust.edu.cn

<sup>1</sup> <https://asd.gsfc.nasa.gov/Koji.Mukai/novae/latnovae.html>

The observed X-ray emission from novae is typically characterized by thermal radiation from the hot WD and/or the shocked matter (Orio et al. 2001; Mukai & Ishida 2001; Mukai et al. 2008; Chomiuk et al. 2014). The soft X-ray emission with an effective temperature of  $< 0.1$  keV can reach a luminosity of  $L_X > 10^{36}$  erg s $^{-1}$ . The soft X-ray emission is thought to originate from a hot WD sustained by residual nuclear burning. As the ejected material spreads out, the surrounding environment becomes optically thin, allowing the soft X-ray emission from the hot WD becomes visible (Page et al. 2020a). The emission in the soft X-ray band defines the Supersoft Source (SSS) phase, when the ejecta became transparent to X-rays from the central source (Bode & Evans 2008). Observations during SSS phase of some novae have confirmed quasi-periodic oscillations (QPOs) with a period in the range of 10 to 100 s (Page et al. 2020b; Beardmore et al. 2019; Ness et al. 2015; Orio et al. 2022). Various possibilities have been suggested: for example, the spin modulation of the WD with a strong magnetic field is the most likely explanation for the QPOs (Drake et al. 2021). Another possibility is the g-mode (buoyancy) pulsations driven by an ionisation-opacity instability, which is expected to produce a period of the order of 10 s or less (Osborne et al. 2011; Drake et al. 2003; Wolf et al. 2018). Consequently, the exact origin of QPO in novae remains unclear.

The nova V1716 Sco (also known as PNV J17224490-4137160; Nova Sco 2023) was discovered by Andrew Pearce on 2023 April 20.678 UT and visually confirmed on April 20.705 UT at magnitude 8.0<sup>2</sup>. Data from the All-Sky Automated Survey for Supernovae (ASAS-SN) revealed a pre-discovery detection on 2023 April 20.410 UT (Sokolovsky et al. 2023), and spectroscopically confirmed as a classical (Fe II) nova (Walter & Pearce 2023; Shore et al. 2023). In this paper we adopt the date of the first ASAS-SN detection as the eruption start time  $t_0 = \text{UT } 2023\text{-}04\text{-}20.410 = \text{JD } 2460054.910 = \text{MJD } 60054.410$ .

Cheung (2023) reported the detection gamma-ray emission ( $> 5\sigma$  significance level) using *Fermi*-LAT data taken from 2023-04-21 00:00:00 to 24:00:00 UTC. The  $>100$  MeV flux averaged over that period was  $F_\gamma = (6.5 \pm 2.1) \times 10^{-7}$  ph cm $^{-2}$ s $^{-1}$  and the photon index= $1.9 \pm 0.2$ . Hard X-rays were detected by NuSTAR on 2023 April 21.89 UT, with the X-ray spectrum being consistent with a heavily absorbed thermal plasma (Sokolovsky et al. 2023). *Swift* detected the X-ray emission on 2023 May 01 and confirmed an additional soft

component appeared after 2023 May 31 (Page & Kuin 2023). Dethero et al. (2023) reported the power spectrum of V1716 Sco using NICER data and confirmed a strong pulsation around a period of  $\sim 80$  s, which may be a SSS QPO as this period appears to be slightly varying.

In this *Letter*, we report results of more detailed GeV and X-ray analyses of nova V1716 Sco. In Section 2, we describe the data analysis conducted by *Swift*, NICER, NuSTAR and *Fermi*-LAT observations. Section 3 is the discussion about the results from the gamma-ray and X-ray data analysis. We make a conclusion in Section 4.

## 2. DATA REDUCTION AND RESULTS

### 2.1. *Fermi*-LAT data

We performed a binned analysis using the standard *Fermi*-LAT ScienceTool package, which is available from the *Fermi*-LAT Science Support Center<sup>3</sup>. We selected Pass 8 data in the energy band of 0.1-300 GeV. The data for the fourth *Fermi*-LAT catalog (4FGL DR4) were taken during the period August 2008 to August 2022 covering 14 years (Ballet et al. 2023; Abdollahi et al. 2022). We conducted a binned analysis using a gamma-ray emission model file based on the 4FGL DR4 catalog. To avoid contamination from Earth's limb, we included only events with zenith angles less than 90 degrees. Our analysis limited the events from the point source or Galactic diffuse class (`event class = 128`) and utilized data from both the front and back sections of the tracker (`evttype = 3`).

For the analysis of the GeV emission from the target, we selected the data with the energy above 100 MeV and the time epoch to cover from MJD 60040, which is  $\sim 15$  days before the detection of its optical eruption (at 2023 April 20.410 = MJD 60054.410), to MJD 60250. We constructed a background emission model that incorporates both the Galactic diffuse emission (`gll_iem_v07`) and the isotropic diffuse emission (`iso_P8R3_SOURCE_V3_v1`) provided by the *Fermi*-LAT Science Support Center. A gamma-ray emission model for the whole ROI was built using all sources in the fourth *Fermi*-LAT catalog (Abdollahi et al. 2020) located within  $20^\circ$  of the nova V1716 Sco, and the target is included in the model at the nova position of (R.A., decl.)=( $17^\circ 22' 44.88''$ ,  $-41^\circ 37' 16.0''$ ).

To describe the TS value and flux time evolution, we conducted a refit of the gamma-ray data in each bin using binned likelihood analysis (*gtlike*). We created a

<sup>2</sup> <http://www.cbat.eps.harvard.edu/unconf/followups/J17224490-4137160.html>

<sup>3</sup> <https://fermi.gsfc.nasa.gov/ssc/data/access/lat/>

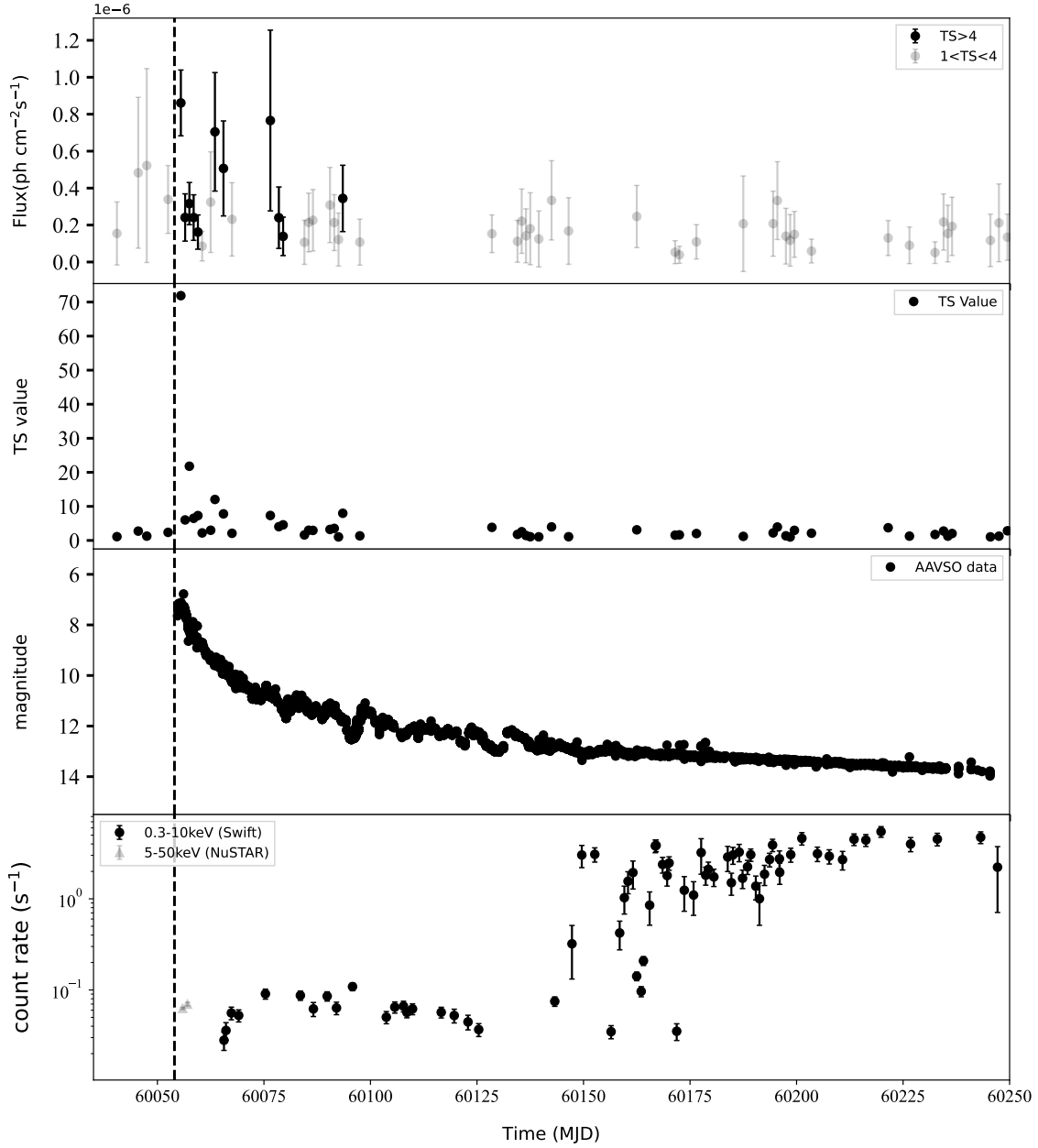


**Figure 1.** The photon flux with 1-day bin using Fermi-LAT data. The black dots and the light black dots in upper panel are the flux with the TS value large than 4 (corresponding to a detection significance of  $\sim 2\sigma$ ) and 1 ( $\sim 1\sigma$ ), respectively. Second panel: the evolution of TS value. Third panel: the AAVSO V-band light curve from optical data in site of <http://aavso.org/lcg>. Fourth panel: the count rate of X-ray data which come from the Swift telescope in 0.3-10.0 keV (blue data), NuSTAR data in 5.0-50.0 keV (light black triangle). The vertical dash line shows the epoch of nova eruption in optical.

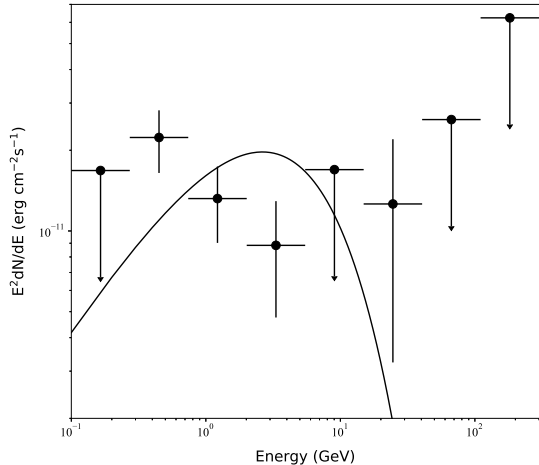


**Figure 2.** The spectrum of V1716 Sco with Fermi-LAT in 0.1-300 GeV band. The black line shows the best-fitting models for spectrum according to the ‘PLSuperExpCutoff’ model as equation 1.

daily light curve to enable us a more precise measurement of the epoch of the gamma-ray emission, as shown in Figure 1. In the daily light curve of Figure 1, the  $TS$  value reached to the maximum value ( $\sim 70$ ), which corresponds to a detection significance level larger  $8\sigma$  (i.e.,  $\sqrt{TS}$  is about detection significance in  $\sigma$ ). After the peak, the  $TS$  value decayed rapidly and the emissions with  $TS > 4$  ( $\sigma > 2$ ) were confirmed until  $\sim 40$  days after the nova eruption.

To generate the spectrum, we performed the likelihood analysis using the data obtained from MJD 60055 to MJD 60094, during which the emission with  $TS > 4$  were confirmed. The gamma-ray spectrum can be well describe by a power-law function with an exponential cut-off, as describe:

$$\frac{dN}{dE} \propto E^{-\gamma_1} \exp \left[ - \left( \frac{E}{E_c} \right)^{\gamma_2} \right], \quad (1)$$

where we fixed to  $\gamma_2 = 2/3$ . We obtained a power-law index of  $\gamma_1 = 1.98(7)$  and a cut-off energy of  $E_c = 22.1(1)$  GeV. We obtained an averaged energy flux of  $F_\gamma = 1.4(1) \times 10^{-11}$  erg  $\text{cm}^{-2} \text{s}^{-1}$  in 0.1-300 GeV bands. Figure 2 represents the spectrum in GeV bands. We also extracted the energy flux for the time bin that has  $TS \sim 70$  and obtained  $F_\gamma \sim 1.4(3) \times 10^{-10}$  erg  $\text{cm}^{-2} \text{s}^{-1}$ .

According to GAIA archive<sup>4</sup>, the distance of nova V1716 Sco is estimated as  $3.16^{+2.13}_{-1.62}$  kpc or  $4.96^{+1.75}_{-1.06}$  kpc in geometric or photogeometric measurements (Bailer-Jones et al. 2021). To estimate the total emitted energy

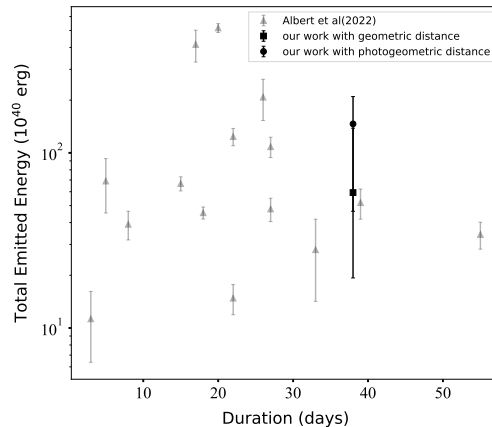


**Figure 3.** Total emitted GeV energy vs. duration of GeV emission of the novae detected in the GeV range. The duration is defined by the epoch during which the emission with  $TS > 4$  lasted. The data illustrated with triangles are taken from Albert et al. (2022). The symbols with the square and filled circles correspond to the emission energy of nova V1716 Sco estimated with the geometric distance and photogeometric distance, respectively.

in the gamma-ray bands, we integrated the daily flux detected with  $TS > 4$  and obtained  $0.59(1) \times 10^{42}$  erg for  $d=3.16$  kpc and  $1.46(7) \times 10^{42}$  erg for  $d=4.96$  kpc. Figure 3 shows the total emitted energy and duration of the gamma-ray emission of GeV novae. It can be seen that the total emission gamma-ray of V1716 Sco is similar to those of other novae detected by *Fermi*-LAT.

## 2.2. NuSTAR data

NuSTAR observed V1716 Sco between 2023-04-21 21:36:56( $t_0 + 1.5$ d) to 2023-04-23 09:54:11 ( $t_0 + 3.0$ d) (ObsID:80801335002) after a day of optical eruption with a total exposure time 65 ks. For the analysis, we used the tasks of `nupipeline` and `nuproducts` to extract source and background spectra and light curves from the focal plane modules A (FPMA) and B (FPMB). We generated the source and background extraction region files using DS9 by choosing a circular region of  $\sim 50''$  radius centered on the source and the background region close to the source, respectively. We grouped the channels at least 30 counts per bin for NuSTAR FPM A/B data. Preliminary analysis of Sokolovsky et al. (2023) suggests that the X-ray spectrum is consistent with that of a heavily absorbed thermal plasma with  $k_B T = 31 \pm 13$  keV with  $k_B$  begin Boltzmann constant, and  $N_H = (82 \pm 15) \times 10^{22} \text{cm}^{-2}$ .

We fit observed spectra of V1716 Sco (Figure 4) with the power-law model (`tbabs*polwerlaw`) or the thermal plasma emission (`tbabs*apec`). For the power-

<sup>4</sup> <https://dc.g-vo.org/gedr3dist/q/cone/form>

law model, we obtain a photon index of  $2.55 \pm 0.83$  and a hydrogen column density of  $N_H = (144.56 \pm 58.14) \times 10^{22} \text{ cm}^{-2}$  (Table 1), which for the thermal plasma emission model,  $k_B T \sim 20.15 \pm 16.13 \text{ keV}$  and  $N_H = (117.02 \pm 44.60) \times 10^{22} \text{ cm}^{-2}$  that are consistent with previous study. We obtained an unabsorbed flux of  $(2 - 3) \times 10^{-12} \text{ erg cm}^{-2} \text{ s}^{-1}$ , as Table 1. During NuSTAR observation, the TS-value of the *Fermi*-LAT observation reached to the maximum value of  $\sim 70$ . It is therefore found that around the GeV peak, the gamma-ray luminosity is about two order of magnitude larger than the radiation luminosity in 5-50 keV bands.

**Table 1.** Spectra parameters of NuSTAR telescope

FPMA/B	PL	APEC
$N_H(10^{22} \text{ cm}^{-2})$	$144.56 \pm 58.14$	$117.02 \pm 44.60$
photon index	$2.55 \pm 0.83$	-
kT(keV)	-	$20.15 \pm 16.13$
C-stat/dof	42/31	43/31
$F^a$	$2.85 \pm 1.02$	$2.09 \pm 0.51$

<sup>a</sup> Unabsorbed flux in 5.0-50.0 keV energy bands ( $10^{-12} \text{ erg cm}^{-2} \text{ s}^{-1}$ ).

### 2.3. *Swift*-XRT data

*Swift* had continuously monitored V1716 Sco since the discovery of the nova eruption. We create the light curve and hardness ratio of the X-ray emission using the XRT web tool<sup>5</sup> (Evans et al. 2007, 2009). We use only grade 0 events in the analysis to minimize the optical loading and eliminate the pile-up effect. The light curves after eliminate the pile-up were shown in the bottom panel of Figure 1 and Figure 5. The hardness ratio (bottom panel of Figure 5) continuously decreased and the observed emission entered SSS phase at around MJD 60095.

To investigate the spectral properties, we downloaded the archival data from HEASARC Browse<sup>6</sup> and performed the analysis with the HEASOFT version 6.31.1 and its SWIFTDAS package with the updated calibration files. The clean event lists were obtained using the task `xrtpipeline` of the HEASOFT and extract the spectrum using `Xselect`. We grouped the source spectra to ensure at least 1 count per spectral bin and fit the spectra using `Xspec`. For the spectral analysis of the *Swift* data, we limit to the data taken before MJD 60130, after which the pile-up effect will be severe. We present

<sup>5</sup> [https://www.swift.ac.uk/user\\_objects/](https://www.swift.ac.uk/user_objects/)

<sup>6</sup> <https://heasarc.gsfc.nasa.gov/cgi-bin/W3Browse/w3browse.pl>

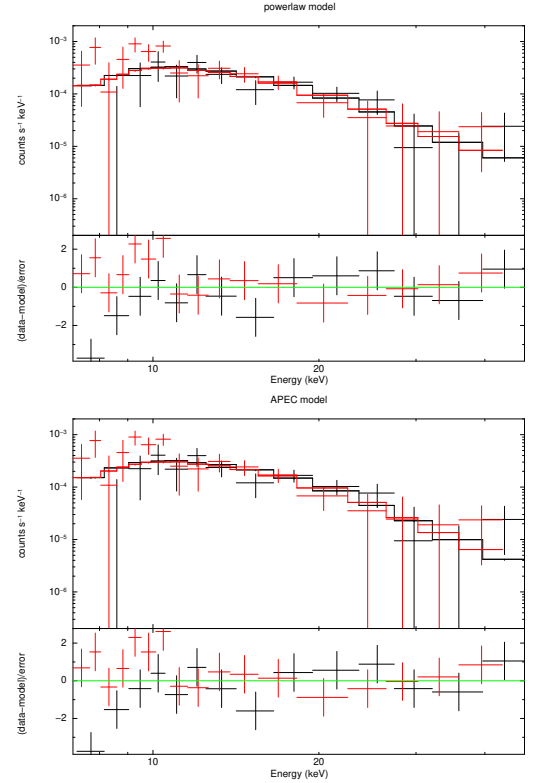


**Figure 4.** Phase-average spectrum in 5.0-50.0 keV, the observed spectra with the FPMA (black spectrum) and FPMB detectors (red spectrum) are simultaneously fitted by an absorbed power-law model(upper) and apec model(lower).

the spectra in SSS phase with the data taken by NICER (section 2.4).

We employed the thermal plasma emission (`apec` model in `Xspec`) to fit the observed spectra. As Table 2 shows, the spectra of the initial stage of the *Swift* observations are fitted by the optically thin thermal plasma emission with a temperature of several keV. It may be reasonable to assume that the component of thermal plasma emission originates from the shocked heated plasma (Steinberg & Metzger 2018),

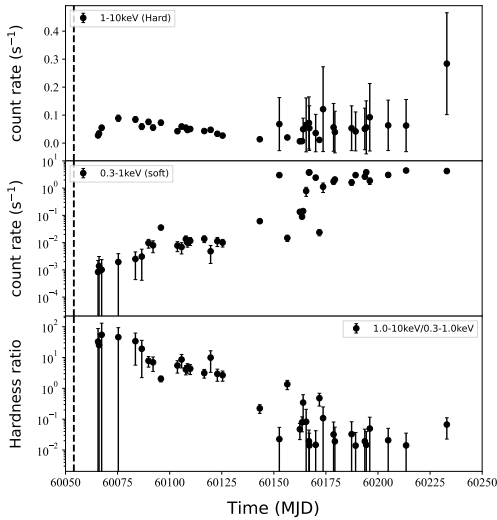
$$k_B T \approx 1.2 \text{ keV} \left( \frac{v}{10^3 \text{ km s}^{-1}} \right)^2, \quad (2)$$

where  $v$  is the shock velocity.

As Figure 1 and 5 show, *Swift*-XRT measured the X-ray evolution in the epoch overlapping with the GeV detection by *Fermi*-LAT. After the first detection, the flux in 1.0-10 keV bands increased rapidly and reached to the local maximum value at about MJD 60075 (about 20 days eruption). We found that the flux in 0.3-10 keV bands around MJD 60075 is  $\sim 1.6 \times 10^{-11} \text{ erg cm}^{-2} \text{ s}^{-2}$ . Comparing the energy flux in GeV bands around MJD 60075, we found that the ratio of the GeV luminosity over the X-ray luminosity

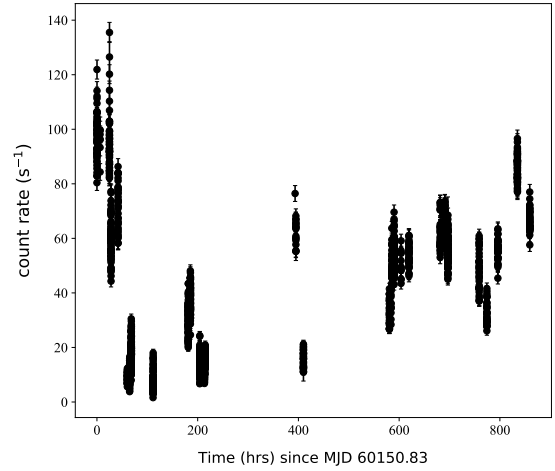
**Table 2.** The parameters of X-ray data from Swift, using the model of BB and apec.

ObsID	date(MJD)	$N_H(10^{22} \text{ cm}^{-2})$	$kT_{apec} \text{ (keV)}$	$F_{apec}^a$	$k_B T_{bb} \text{ (eV)}$	$F_{bb}^a$	$R_{bb}(10^3 \text{ km})$	C-Stat/dof
00015990004	60066	$4.42 \pm 1.64$	$4.56 \pm 5.15$	$0.91 \pm 0.064$	-	-	-	34/34
00016007006	60067	$6.95 \pm 2.03$	$2.33 \pm 0.80$	$1.16 \pm 0.32$	-	-	-	46/42
00016007014	60075	$2.33 \pm 0.56$	$2.41 \pm 0.81$	$1.57 \pm 0.31$	-	-	-	57/64
00016023006	60089	$1.57 \pm 0.42$	$1.90 \pm 0.47$	$1.01 \pm 0.21$	-	-	-	62/55
00016023010	60095	$0.78 \pm 0.18$	$2.75 \pm 0.93$	$0.56 \pm 0.10$	$28.85 \pm 7.10$	$0.67 \pm 0.58$	$35.32 \pm 57.96$	90/89
00016066006	60105	$0.57 \pm 0.19$	$2.59 \pm 0.70$	$0.38 \pm 0.11$	-	-	-	43/48
00016066010	60107	$1.28 \pm 0.43$	$1.42 \pm 0.35$	$0.67 \pm 0.14$	$54.02 \pm 12.53$	$3.14 \pm 1.61$	$4.60 \pm 12.13$	52/49
00015990006	60116	$1.10 \pm 0.37$	$1.37 \pm 0.26$	$0.46 \pm 0.11$	$48.50 \pm 9.62$	$16.59 \pm 7.55$	$6.00 \pm 12.28$	46/53
00015990008	60122	$0.73 \pm 0.64$	$3.13 \pm 2.00$	$0.26 \pm 0.077$	$88.93 \pm 38.97$	$0.098 \pm 0.047$	$0.092 \pm 0.33$	34/44

<sup>a</sup>The unabsorbed flux is measured in 0.3-10.0 keV and recorded in units of  $10^{-11} \text{ erg cm}^{-2} \text{ s}^{-1}$ .**Figure 5.** The light curves of hard X-rays (top panel) and soft X-rays (middle panel) from Swift when consider pile up effect. The bottom panel shows the hardness ratio (1.0-10.0 keV/0.3-1.0 keV)(bottom panel).

(0.3-10 keV bands) is  $L_\gamma/L_x \sim 100$ , which is typical value for nova detected in GeV bands (see Figure 5 of Gordon et al. (2021)).

After the local peak, the X-ray count rate in the hard band (1.0-10 keV bands) and the hardness decreased, while the count rate in soft bands (0.3-1.0 keV bands) rapidly increases, as Figure 5 shows. The spectra after the peak is required the BB component, as Table 2 indicates. Although we cannot constrain the radius of the emission region, the temperature of  $\sim 50$  eV suggests the thermal emission from the WD surfaces. As the light curve in Figure 5 shows, the observed X-ray emission enters the SSS phase about 40 days after the nova eruption.

**Figure 6.** Light curve of nova V1716 Sco observed with NICER with 10 s time bins, on 2023 July 25 to 2023 August 30.

#### 2.4. NICER data

Neutron Star Interior Composition Explorer (NICER) observed the target in SSS phase and covered from three month to fourth month after the optical eruption. We apply the standard task `nicer112` to extract the cleaned event file and perform the barycentric time correction using the `barycorr` task of `HEASoft`. Figure 6 presents the light curve of whole NICER and Figure 7 show the light curves of two data sets. In Figure 7, we can clearly confirm a periodic modulation with a period of  $\sim 80$  s, as reported by Dethero et al. (2023).

We search for the periodic modulation in the light curve (10 s time bin) in each data set and confirmed the significant signal from 14 data sets (Table 3). Combining these 14 data sets, we obtained the period of  $79.10 \pm 1.98$  s in Lomb-Scargle (LS) periodogram (top panel of Figure 8). As Table 3 shows, since the periods



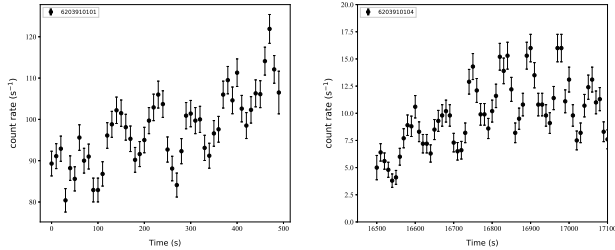


**Figure 7.** Light curve of nova V1716 Sco observed by NICER with 10 s time bins on obsID 6203910101 (left) and 6203910104 (right) in 0.2–10.0 keV. These two examples illustrating how the modulation with the 80 s period is evident even visually. X-axis shown the time since observations beginning.

**Table 3.** The results from LS periodogram of each NICER data in full energy.

ObsID	Start time(MJD)	Exposure(s)	Period(s)
6203910101	60150.83	494	80.33±4.25
6203910103	60151.99	1077	75.69±7.23
6203910104	60153.34	2635	77.98±4.76
6203910109	60158.38	1619	77.94±6.09
6203910110	60159.33	1724	76.76±5.79
6203910112	60167.22	529	76.84±10.36
6203910113	60168.04	1130	77.88±7.30
6203910117	60175.02	1696	79.08±6.01
6203910118	60175.99	502	76.02±10.64
6203910121	60179.22	1683	78.57±8.52
6203910123	60182.45	435	78.41±11.72
6203910124	60183.09	326	78.79±13.71
6203910125	60184.00	402	77.50±12.10
6203910126	60185.61	536	80.40±10.94

obtained with different data sets are consistent within the error, we could not confirm temporal evolution of the period in LS periodogram. The folded pulse profile can be described by a single broad peak, as the bottom panel of Figure 8 shows; we present the pulse profile of each data set folded with 79.10 s in Appendix (Figure A1). To investigate the stability of position of the pulse peak in the folded light curve, we fit the individual pulse profile folded by 79.10 s with a Gaussian function and obtain the fitting parameters with the Monte Carlo method. We find that the position of the pulse peak indicates a rapid temporal variation, as Figure 9 shows. This variation of the peak phase makes difficult to create an ephemeris of the period evolution. It is probability that the period of the modulation is not stable with time because the hot spot region on the WD’s surface may shift with time or the periodic modulation may be

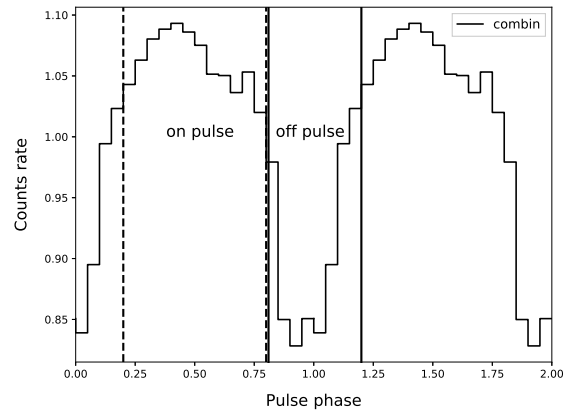
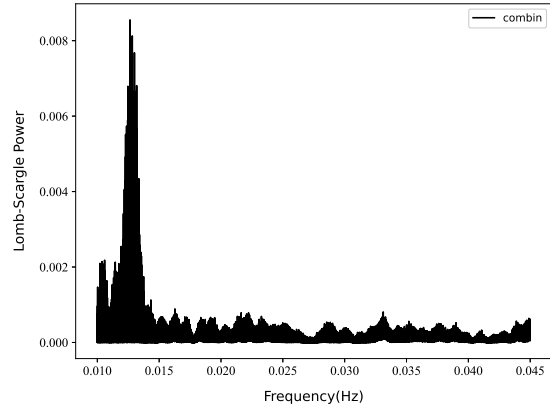


**Figure 8.** The LS periodogram by Combining the data sets shown in Table 3(upper), a peak with period of  $79.10 \pm 1.98$  second. Folded pulse profile from the result of LS periodogram(bottom). The vertical dashed lines and solid lines define the on- and off-pulse phases, respectively.

originated from the different mechanism (e.g. g-mode oscillation).

Because of its high-timing resolution of NICER, the effect of the pile-up with a count rate of  $\sim 10^2 \text{ s}^{-1}$  is not serious problem, comparing to the data of the *Swift* (Orio et al. 2023). To investigate the emission of the pulsed component, we carried out the phase-resolved spectroscopy. We extract the spectra of the on-pulse and off-pulse phase, which are indicated in Figure 8, and the spectrum of the pulsed component by extracting the spectrum of the off-pulse phase from that of the on-pulsed phase (Figures 10 and A2). The spectra can be well fitted by the BB radiation with a temperature of 30 – 40 eV (Table 4), which is typical value in SSS phase of the novae. The hydrogen column density is  $N_H = (0.5 - 0.8) \times 10^{22} \text{ cm}^{-2}$  and did not show a large temporal evolution. As the fifth and sixth columns of Table 4 show, the X-ray emission in SSS phase exceeds the Eddington luminosity with an emission size of

$R_{bb} \sim 10^{10}$  cm, for which we assume a typical distance of 4kpc. With the assumption of the BB radiation, the super Eddington luminosity had been observed for about 30 days and until  $\sim 130$  days after the optical eruption.

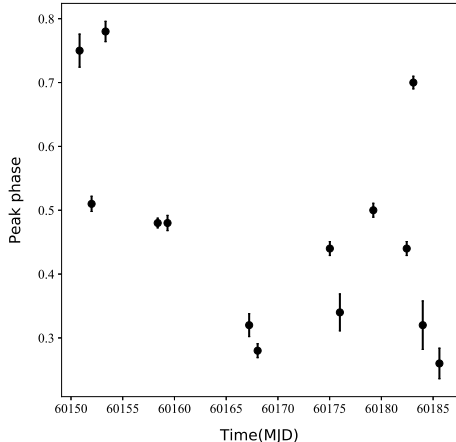


**Figure 9.** The peak phase with time evolution observed by NICER.

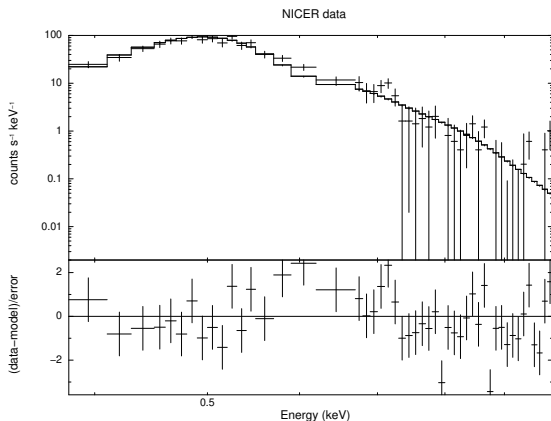


**Figure 10.** Phase resolve spectrum of NICER data

### 3. DISCUSSION

As shown in Table 4 and Figure 11, the BB temperature and the radius of hot spot exhibit an anti-correlation. Krautter et al. (1996) reported the residual material is hot when the X-ray emission from a fading post-eruption nova, the radius of hot spot begins shrink, and, consequently, the BB temperature rises. As Table 4 shows, on the other hand, the bolometric luminosity estimated from the BB fits in SSS exceeds the Eddington luminosity of  $L_{edd} \sim 1.5 \times 10^{38}$  ergs  $s^{-1}$  for a solar mass object. Some novae, such as RS Oph and SMCN 2016-10a, have also exhibited such a super Eddington emis-

sion with the BB model (Aydi et al. 2018; Page et al. 2022). Kato & Hachisu (2005) has proposed that during the super-Eddington phase of a nova, the envelope develops a porous structure and this porosity significantly reduces the effective opacity of the atmosphere. Krautter et al. (1996), on the other hand, discussed that BB models for the emission from a hot WD can overestimate the luminosity and the super-Eddington radiation should not be considered physically realistic. Instead, only the comparative trends should be taken into account (Page et al. 2022).

As Figure 5 shows, the significant detection of the hard X-ray (1-10 keV) bands of the *Swift* observation started at about 10 days after the optical eruption, at which gamma-ray emission was still detected. Figure 3 in Gordon et al. (2021) illustrated the evolution of X-ray emission over time since the discovery of several *Fermi*-LAT-detected 10 classical novae. It shows that a significant detection of *Swift* X-rays emission started only after the gamma-ray emission disappeared. There were some novae with a companion of red giant have been detected the X-ray emission (1-10 keV) and GeV emission concurrently. Such as nova V407 Cyg, which has been observed in both gamma-rays and *Swift* X-rays, simultaneously; however, its companion star is a red giant, resulting in an external shock, and the absorbed column is never higher than  $10^{23}$   $cm^{-2}$ . The non-detection of X-ray emissions (1-10 keV) during gamma-ray emissions detected in classical novae maybe due to a combination of large column densities ahead of the shocks, which absorb the X-rays, and the suppression of X-rays by corrugated shock fronts. As shown in Table 1, the harder X-ray emission (above 10 keV) detected after a day of optical eruption with the column density of several  $\times 10^{23}$   $cm^{-2}$ . While in Table 2, the column densities of a few  $\times 10^{22}$   $cm^{-2}$  were detected by *Swift*-XRT after approximately 10 days of optical eruption, during which the gamma-ray emission persisted with approximately  $\sim 2 \sigma$  significance. This indicates that the expanding ejecta exhibit a decrease in column density.

Vurm & Metzger (2018) reported that the shock associated with the nova eruption can accelerated high-energy particles responsible for the gamma-ray emission that extend down to the *NuSTAR* band. *NuSTAR*, operating within the 3-79 keV band, has detected harder X-ray emission simultaneously with gamma-rays in three novae: V5855 Sgr, V906 Car, and YZ Ret (Nelson et al. 2019; Sokolovsky et al. 2020, 2022). Nova V1716 Sco will be the fourth one that has detected harder X-ray emission simultaneously with gamma-rays. We found that the hard X-ray emission (above 10 keV) from *NuSTAR* and the GeV emission from *Fermi*-LAT



**Table 4.** The parameters of X-ray data from NICER, using the model of BB.

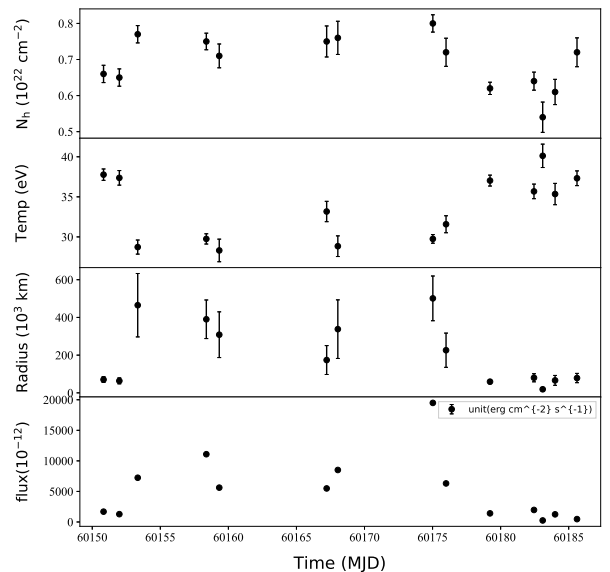
ObsID	Start time(MJD)	$N_H(10^{22} \text{ cm}^{-2})$	$k_B T_{bb}$ (eV)	$R_{bb}(10^3 \text{ km})$	$L(10^{38} \text{ ergs s}^{-1})$	C-Stat/dof
6203910101	60150.83	0.66±0.024	37.77±0.71	70.36±15.29	3.06±1.21	95/55
6203910103	60151.99	0.65±0.024	37.37±0.91	63.57±15.73	2.31±0.47	43/22
6203910104	60153.34	0.77±0.024	28.73±0.88	464.82±168.15	13.10±0.74	26/36
6203910109	60158.38	0.75±0.023	29.75±0.64	390.19±102.34	20.06±5.01	35/19
6203910110	60159.33	0.71±0.033	28.31±1.41	308.40±121.28	10.16±0.85	32/31
6203910112	60167.22	0.75±0.043	33.17±1.27	173.97±76.65	9.93±0.86	55/29
6203910113	60168.04	0.76±0.046	28.84±1.29	337.78±155.41	15.39±2.55	26/25
6203910117	60175.02	0.80±0.024	29.75±0.54	501.07±118.58	35.26±9.71	198/41
6203910118	60175.99	0.72±0.039	31.58±1.06	226.03±90.79	11.41±1.88	88/41
6203910121	60179.22	0.62±0.017	37.03±0.68	59.37±10.93	2.55±0.52	72/30
6203910123	60182.45	0.64±0.025	35.68±0.91	80.09±21.56	3.56±0.99	73/31
6203910124	60183.09	0.54±0.042	40.12±1.46	18.91±9.60	0.45±0.28	16/24
6203910125	60184.00	0.61±0.035	35.35±1.33	66.13±26.19	2.26±1.32	39/31
6203910126	60185.61	0.72±0.040	37.32±0.92	78.58±24.58	0.85±0.36	42/38

were detected on the same day followed optical eruption by one day. The flux in 5-50 keV bands from NuSTAR is  $\sim 2.5 \times 10^{-12} \text{ erg cm}^{-2} \text{ s}^{-1}$ , energy flux of  $F_\gamma \sim 1.4(3) \times 10^{-10} \text{ erg cm}^{-2} \text{ s}^{-1}$  in GeV bands was obtained at the same day (TS $\sim$ 70). The ratio of the GeV luminosity over harder (5-50 keV) X-ray luminosity is around 100. The simultaneous detection of X-ray emissions with transient gamma-rays allows for the quantification of the properties of internal shocks and even the verification of internal shock models.

Nova V1716 Sco is one of rare samples that show the significant detection by *Swift* during the gamma-ray detection, and featuring a 79.10 seconds quasi-periodic oscillation detected by NICER. A oscillations with period of  $79.10 \pm 1.98$  seconds are preferentially observed in SSS phase around 95 days after the optical eruption, a single broad peak pulse obtained and with variations in peak phase. The spin modulation of the WD is the most likely explanation for the QPO, however, the period of the modulations is not stable with time, the hot spot region on the WD's surface may shift with time or the periodic modulation may be originated from the different mechanism, such like a stellar oscillation.

#### 4. SUMMARY

We conducted a joint analysis of NuSTAR, *Swift*, NICER, and *Fermi*-LAT observations of nova V1716 Sco. We confirmed the gamma-ray emissions emerged at a day after the optical eruption with a TS value of 70. The duration of gamma-ray activity with a TS value above 4 lasted for 40 days. Harder X-ray emission was observed by NuSTAR at a day after the optical eruption. We fitted the spectrum with a power-law model with a photon-index of  $2.55 \pm 0.83$  or optically thin

**Figure 11.** The evolution of blackbody temperature, hotspot radius and flux with NICER data.

thermal plasma emission (apec) with a temperature of  $20.15 \pm 16.13 \text{ keV}$ . The significant detection of the hard X-ray emission from *Swift*-XRT was confirmed during the detection of the GeV emission by the *Fermi*-LAT. V1716 Sco will be the first example for classical nova, in which the X-ray detection by *Swift*-XRT is concurrent with gamma-ray emission. The X-ray spectrum taken by *Swift*-XRT just after the emergence was fitted by an emission from the thermal plasma, which likely originates from the shock. The hardness ratio rapidly de-

creased over time, and the observed emission entered the SSS phase at  $\sim 40$  days after the nova eruption. Using the NICER observation, we find that the BB fit predicts the super Eddington luminosity, which are also observed in other novae. We reconfirmed the periodic oscillation with a period of  $79.10 \pm 1.98$  s in SSS phase, which is consistent with the result reported in Dethero et al. (2023). We found that the phase location of the pulse peak is not stable with time.

## ACKNOWLEDGEMENTS

We acknowledge with thanks the variable star observations from the AAVSO International Database contributed by observers worldwide and used in this research. This work made use of data supplied by the UK Swift Science Data Centre at the University of Leicester. J.T. is supported by the National Key Research and Development Program of China (grant No. 2020YFC2201400) and the National Natural Science Foundation of China (grant No. 12173014). L.C.-C.L. is supported by NSTC through grants 110-2112-M-006-006-MY3 and 112-2811-M-006-019.

Facilities: Fermi, NuSTAR, Swift, NICER.

## REFERENCES

- Abdollahi, S., Acero, F., Ackermann, M., et al. 2020, *ApJS*, 247, 33
- Abdollahi, S., Acero, F., Baldini, L., et al. 2022, *ApJS*, 260, 53
- Acciari, V. A., Ansoldi, S., Antonelli, L. A., et al. 2022, *Nature Astronomy*, 6, 689
- Albert, A., Alfaro, R., Alvarez, C., et al. 2022, *ApJ*, 940, 141
- Aydi, E., Orio, M., Beardmore, A. P., et al. 2018, *MNRAS*, 480, 572
- Aydi, E., Chomiuk, L., Izzo, L., et al. 2020, *ApJ*, 905, 62
- Bailer-Jones, C. A. L., Rybizki, J., Fouesneau, M., Demleitner, M., & Andrae, R. 2021, *AJ*, 161, 147
- Ballet, J., Bruel, P., Burnett, T. H., Lott, B., & The Fermi-LAT collaboration. 2023, arXiv e-prints, arXiv:2307.12546
- Beardmore, A. P., Page, K. L., Markwardt, C. B., et al. 2019, *The Astronomer's Telegram*, 13086, 1
- Bode, M. F., & Evans, A. 2008, *Classical Novae*, Vol. 43
- Cheung, C. C. 2023, *The Astronomer's Telegram*, 16002, 1
- Chomiuk, L., Metzger, B. D., & Shen, K. J. 2021, *ARA&A*, 59, 391
- Chomiuk, L., Linford, J. D., Yang, J., et al. 2014, *Nature*, 514, 339
- Della Valle, M., & Izzo, L. 2020, *A&A Rv*, 28, 3
- Dethero, M. G., Charles, E., Hare, J., et al. 2023, *The Astronomer's Telegram*, 16167, 1
- Drake, J. J., Wagner, R. M., Starrfield, S., et al. 2003, *ApJ*, 584, 448
- Drake, J. J., Ness, J.-U., Page, K. L., et al. 2021, *ApJL*, 922, L42
- Evans, P. A., Beardmore, A. P., Page, K. L., et al. 2007, *A&A*, 469, 379
- . 2009, *MNRAS*, 397, 1177
- Gallagher, J. S., & Starrfield, S. 1978, *ARA&A*, 16, 171
- Gordon, A. C., Aydi, E., Page, K. L., et al. 2021, *ApJ*, 910, 134
- H. E. S. S. Collaboration, Aharonian, F., Ait Benkhali, F., et al. 2022, *Science*, 376, 77
- Kato, M., & Hachisu, I. 2005, *ApJL*, 633, L117
- Krautter, J., Oegelman, H., Starrfield, S., Wichmann, R., & Pfeffermann, E. 1996, *ApJ*, 456, 788
- Metzger, B. D., Hascoët, R., Vurm, I., et al. 2014, *MNRAS*, 442, 713
- Mukai, K., & Ishida, M. 2001, *ApJ*, 551, 1024
- Mukai, K., Orio, M., & Della Valle, M. 2008, *ApJ*, 677, 1248
- Nelson, T., Mukai, K., Li, K.-L., et al. 2019, *ApJ*, 872, 86
- Ness, J. U., Beardmore, A. P., Osborne, J. P., et al. 2015, *A&A*, 578, A39
- Orio, M., Covington, J., & Ögelman, H. 2001, *A&A*, 373, 542
- Orio, M., Gendreau, K., Giese, M., et al. 2022, *ApJ*, 932, 45
- . 2023, *ApJ*, 955, 37
- Osborne, J. P., Page, K. L., Beardmore, A. P., et al. 2011, *ApJ*, 727, 124
- Page, K. L., Beardmore, A. P., & Osborne, J. P. 2020a, *Advances in Space Research*, 66, 1169
- Page, K. L., & Kuin, N. P. M. 2023, *The Astronomer's Telegram*, 16069, 1
- Page, K. L., Kuin, N. P. M., Beardmore, A. P., et al. 2020b, *MNRAS*, 499, 4814
- Page, K. L., Beardmore, A. P., Osborne, J. P., et al. 2022, *MNRAS*, 514, 1557
- Shore, S., Charbonnel, S., Le Du, P., et al. 2023, *The Astronomer's Telegram*, 16004, 1
- Sokolovsky, K., Aydi, E., Chomiuk, L., et al. 2023, *The Astronomer's Telegram*, 16018, 1
- Sokolovsky, K. V., Mukai, K., Chomiuk, L., et al. 2020, *MNRAS*, 497, 2569
- Sokolovsky, K. V., Li, K.-L., Lopes de Oliveira, R., et al. 2022, *MNRAS*, 514, 2239

Steinberg, E., & Metzger, B. D. 2018, *MNRAS*, 479, 687

Vurm, I., & Metzger, B. D. 2018, *ApJ*, 852, 62

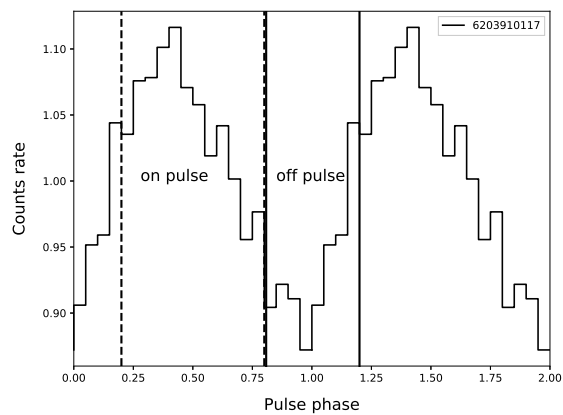
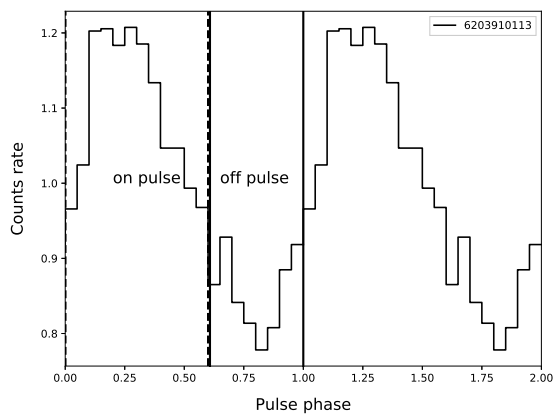
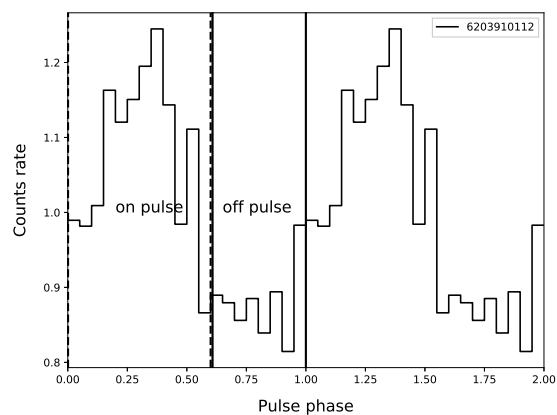
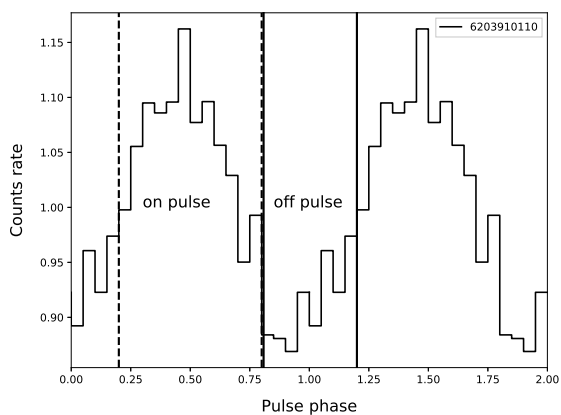
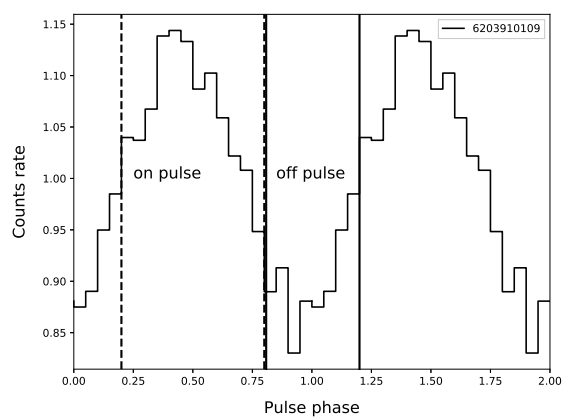
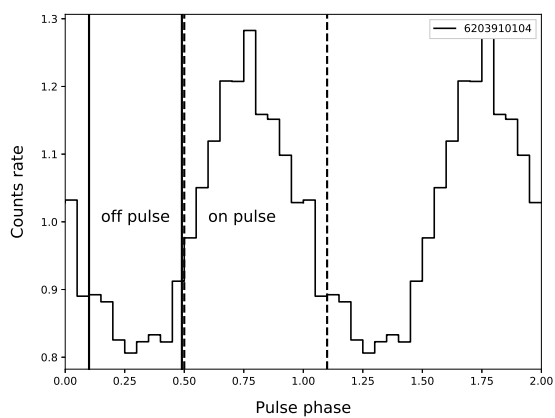
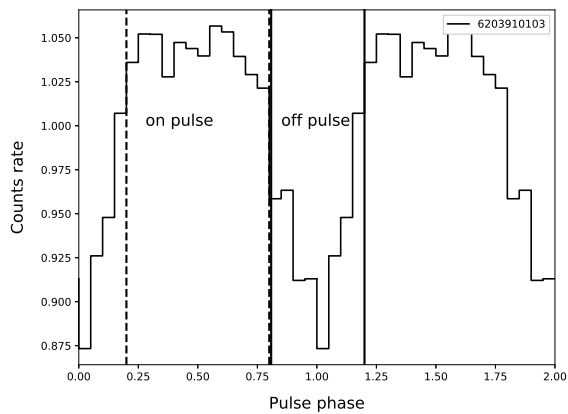
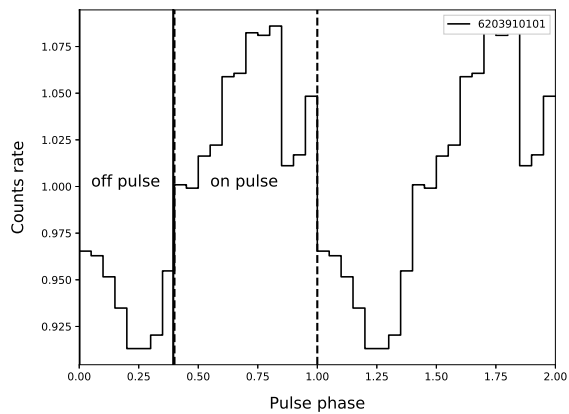
Walter, F. M., & Pearce, A. 2023, *The Astronomer's Telegram*, 16003, 1

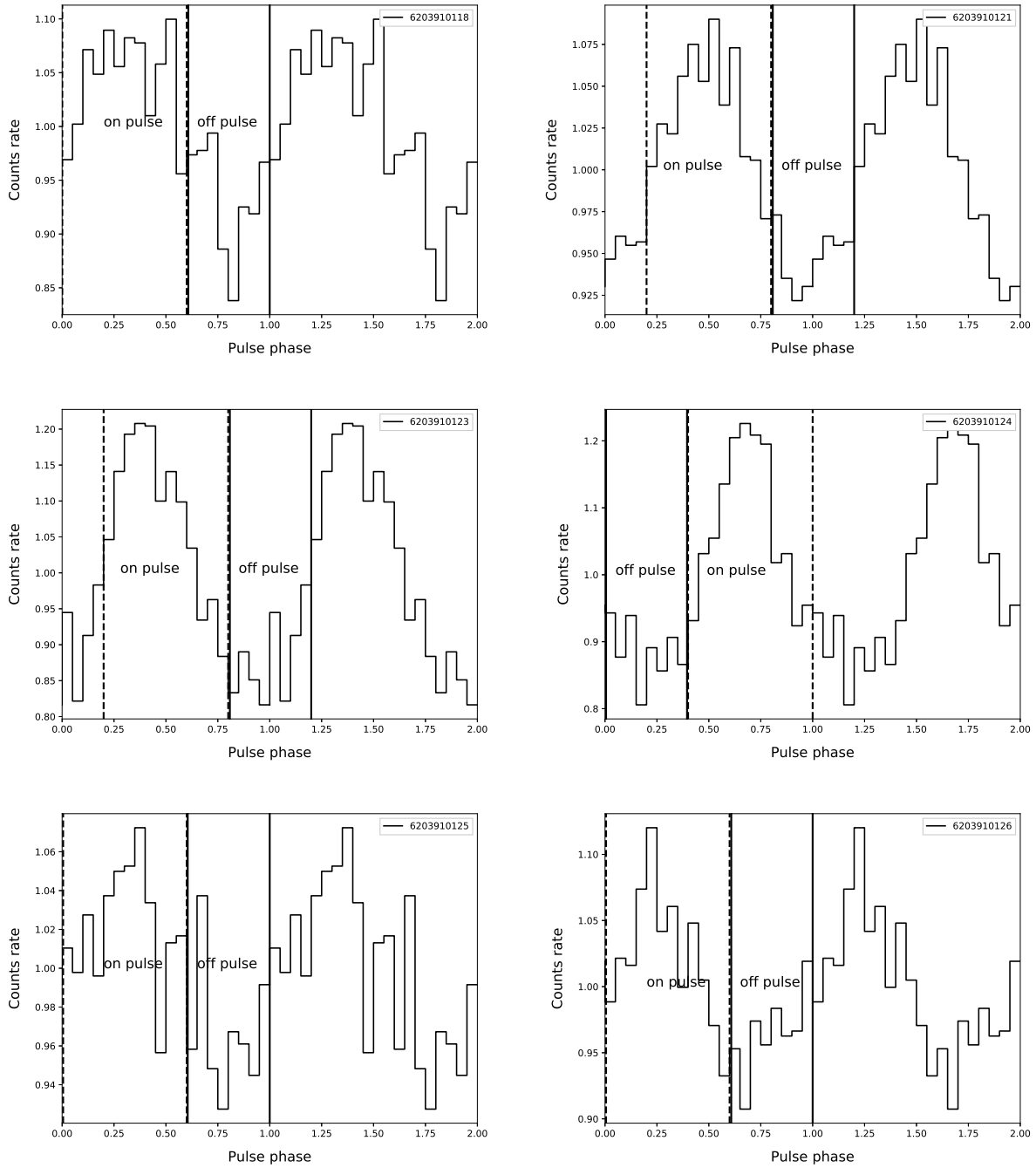
Wolf, W. M., Townsend, R. H. D., & Bildsten, L. 2018, *ApJ*, 855, 127

## APPENDIX

## A. THE PULSE PROFILE FROM NICER DATA

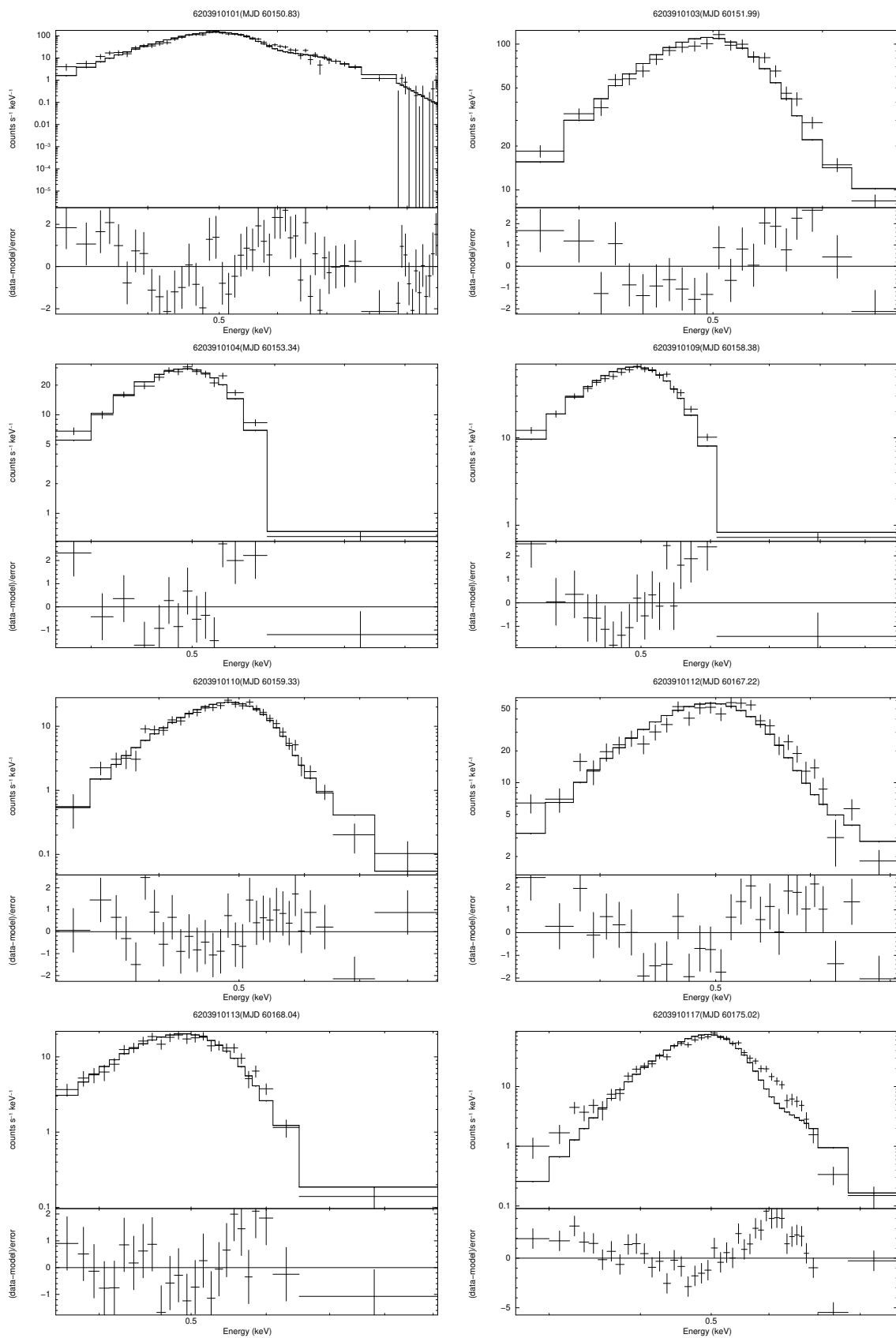
Figure A1 shown the pulse profile using the period of 79.10 obtained from LS periodogram, the vertical dashed and solid lines define the on and off pulse phases. Figure A2 shown the phase-resolve spectra with the off and on phase data, we use a thermal BB (`bodyrad`) with the temperature of  $\sim 30\text{-}40$  eV and a neutral H absorption(`tbabs`) with the column density of  $N_H \sim (0.5\text{-}0.8) \times 10^{22} \text{cm}^{-2}$  to fit the spectra, all the spectral parameters are shown in Table 4.





**Figure A1.** The fold pulse profile using the period get from all the NICER data sets list in Table 3, the period from LS periodogram is 79.10 second. The vertical solid lines and dashed lines define the on- and off-pulse phases, respectively.





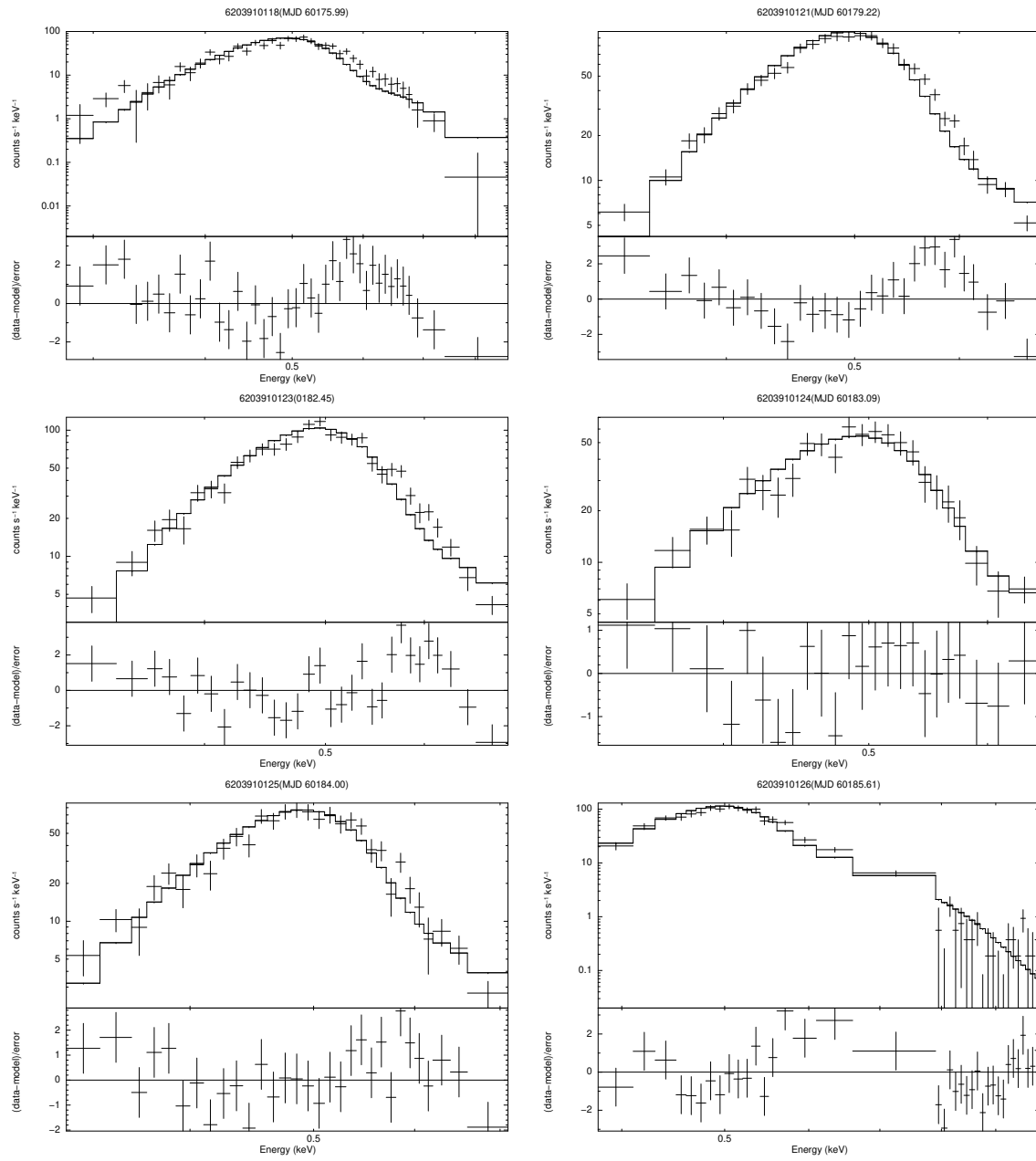


**Figure A2.** The phase resolve spectra of each data sets.